Dependence of vortex breakdown on angular momentum parameter in draft tube flows

C. L. Sharma, S. Soundranayagam, Somkrishan and T. S. Mukund

Department of Mechanical Engineering, Indian Institute of Science, Bangalore 560 012, India

The present study has shown that a rotating runner is a powerful means of investigating draft tube flows because of the convenience in using the hot wire anemometry. A rotating runner acts as a powerful mixing device giving good pressure recovery even in the presence of considerable inlet swirl. Spectrum analysis of the hot wire signal reveals the phenomenon similar to vortex breakdown that introduces oscillations outside a narrow range of unit speed surrounding the design point. There is every indication that water turbine surge and the oscillations observed in the present experiments are one and the same. There is also some evidence that classical vortex break down may not be identical to what happens in the draft tube.

IN water turbine operation, particularly at off-design conditions, the efficiency of the turbine drops down considerably. The machine operation becomes unsteady, resulting in large periodic pressure, power oscillations, harmful vibrations and noise. However, the drop in efficiency is attributed to hydraulic losses, the pressure and power oscillations are often attributed to the eccentric rotation of a vortex core, which forms due to the high inlet swirl in the draft tube. Another feature of operation of turbine at small part load results in pressure surging, at certain conditions it is so violent as to shut down of the turbine becomes inevitable. This pressure surging in water turbines, associated with flow oscillations in the draft tubes may be related to the vortex break down phenomenon in a swirling flow leaving the runner[1]. The vortex break down phenomenon has been studied in connection with swirling flows in pipes and aircraft wings. However, there is very little data on turbine draft tube combinations. But the analysis of vortex break down is difficult in draft tubes compared to pipes, as the flow is in a bent diffuser with swirl. This has resulted in the neglect of the influence of some parameters like swirl distribution. There is no information available in terms of the flow parameters, on the occurrence of vortex breakdown and the onsetting of surging in the water turbine draft tube system, due to the complex nature of the swirl leaving the runner. Complex in the sense that it does not show any standard pattern. The phenomenon of surging was studied in detail by Cassidy[1] and Cassidy and Falvey[2], Hall[3], Harvey[4], Sarpkaya[5], Soundranayagam and Mehta[6], Squire[7], Palde[8], Soundranayagam and Sharma[9] and others. They have shown from their analysis that the swirl at the runner exit is fully responsible for the draft tube surging, and the vortex core results from it. In this paper, we have tried to make an attempt to relate the phenomenon mainly to the angular momentum parameter as a representative of swirl.

The experiments were conducted on the draft tube, using a facility of low speed wind tunnel, available in the turbomachine laboratory of the Department of Mechanical Engineering. The layout of the test rig is shown in Figure 1. This is an open circuit wind tunnel, powered by a centrifugal blower, driven by a 10 HP D. C. motor. The flow rate through the tunnel could be varied by controlling the speed of the motor driving the blower. The blower delivers the air into a diffuser 1.8 m long with an expansion angle of about 10°, the flow enters into a settling chamber of square cross section (1 m × 1 m × 0.9 m). The settling chamber is fitted with honeycombs containing PVC tubes 25 mm in diameter and 150 mm long. The PVC tubes are arranged in layers one above the other and stuck to each other with araldite, the whole structure is rigid and compact and remains in place during the tunnel operation. At the end of the settling chamber is attached a wooden nozzle as per BS 1042, which provides a uniform entry of flow to the inlet duct. The accelerated flow through the inlet duct runs the turbine. A turbine runner assembly (Figure 2) is used to provide the swirl at the draft tube entry. The runner is made of brass and has five blades, with hydrofoil profile and a hub to tip ratio of 0.5. The radial variation of the absolute flow angle approaching the runner is shown in Figure 3. The aerodynamic model of the runner was designed for optimum performance to operate at 7000 rpm, with a pressure drop of 50 mm of water across it. It is a scaled down model of the actual turbine installed in Karnataka. It is located in an aluminium duct 210 mm long and 150 mm in diameter. The speed of the runner is controlled by a hand-operated mechanical brake, and measured electromagnetically.

The draft tube was made as an epoxy shell laminated over a wooden case. The wooden case was built over an aluminium keel on which transverse formers were fixed

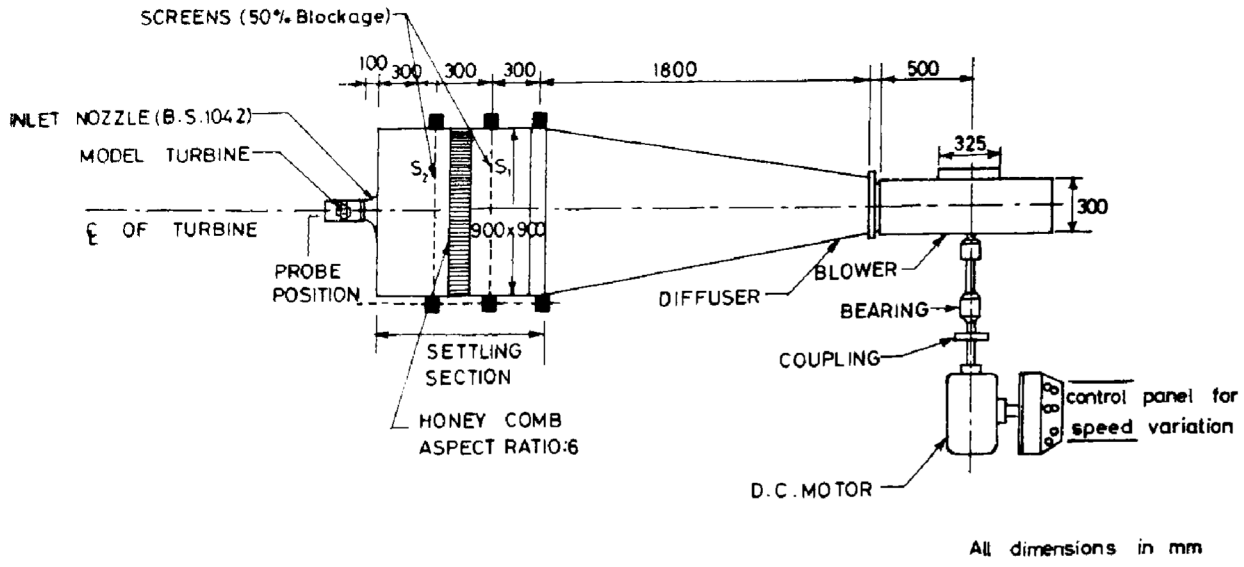

Figure 1. Layout of test rig.

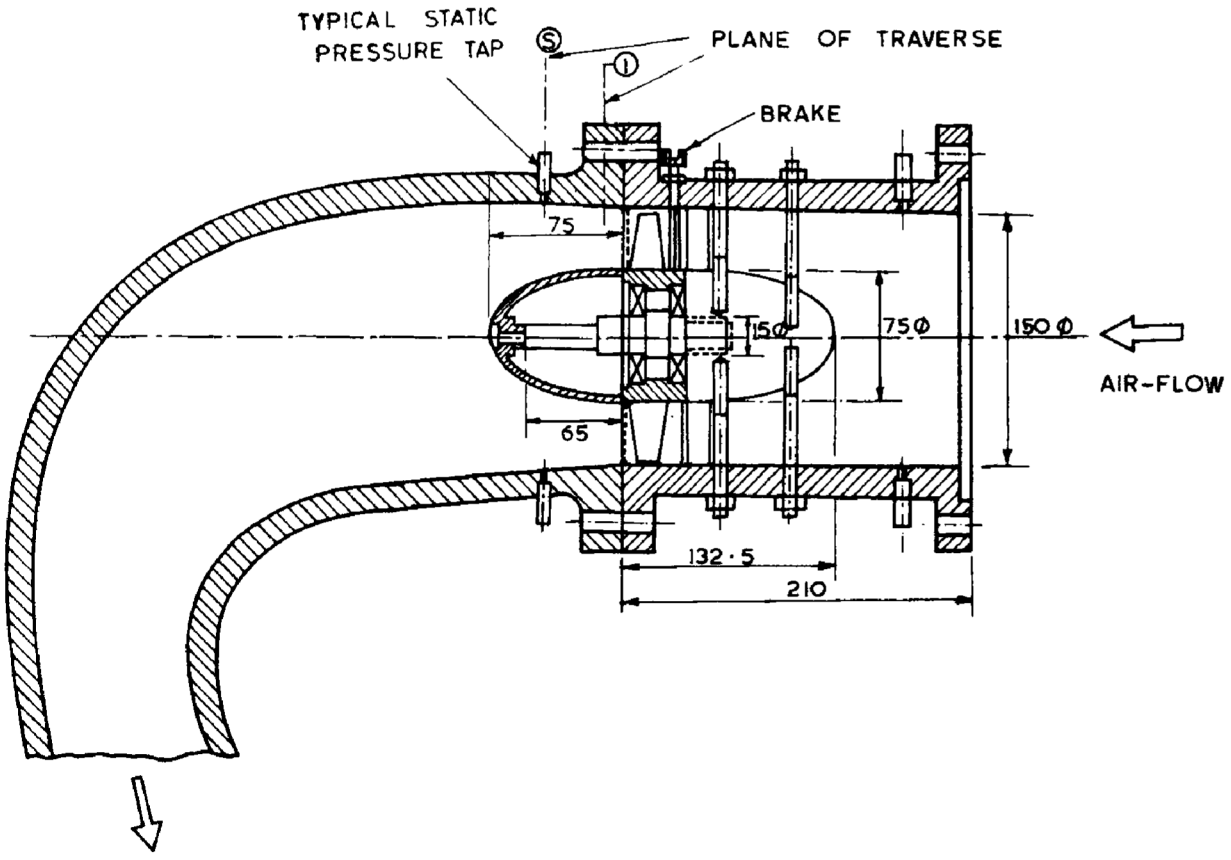

Figure 2. Layout of turbine runner draft tube inlet.

at different stations. The space between the formers was filled with wood and made flush with the formers and the whole unit was polished, The shell was laminated over the separated core in two halves split along the centre of the side walls. The parting as well as the inlet and the outlet were provided with substantial flanges to join the two halves together and to make whole structure rigid. The inside surface of the draft tube shell has an

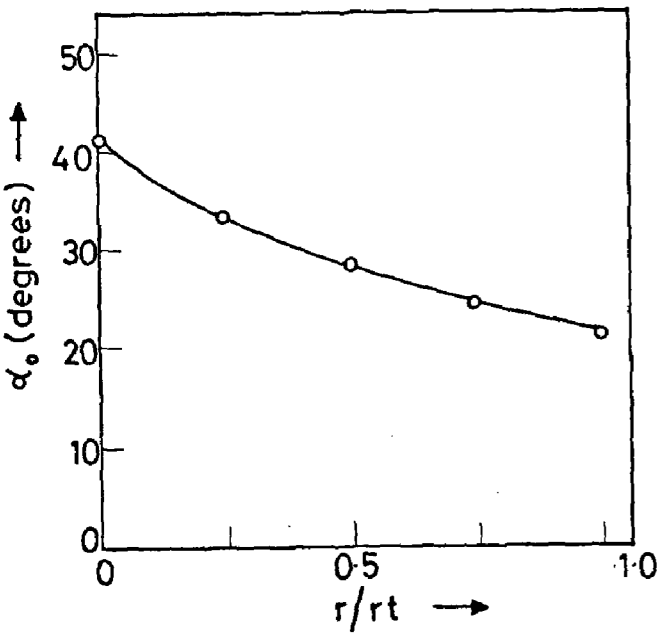

Figure 3. Variation of flow inlet angle from hub to tip.

excellent finish. The elevation and the plan of the draft tube are shown in Figure 4 *a*, *b*. To measure the wall static pressure at the exit of the runner and along the draft tube surface, static pressure taps of diameter 0.5 mm and opening out to take 6 mm diameter adapters, were provided at appropriate traverse stations as shown in Figure 2. Projection type manometers using butyl alcohol (specific gravity 0.8) as the manometric liquid was used to measure the static pressure, the least count of the manometer being 1 mm. To measure the total head, a 1 mm diameter pitot tube squeezed to an oval shape at the measuring end was used. The conventional pitot tube manometer has a very slow response and is incapable of measuring rapid flow fluctuations. Hot wire anemometer responds quickly to rapid fluctuations encountered in the flow. A constant temperature type hot wire anemometer was used. The cold resistance of the wire was 9 ohm, and the overheat ratio of the hot wire anemometer used was 1.67. Since the instrument had a fixed overheat ratio, a tungsten wire having resistance 9 ohm and diameter of 5 micron was used. The anemometer was used in the linearized mode. Flow oscillations were analysed using an FFT analyser. Specifications of the ONO-SOKKI CF-900 series FFT analyser are as follows:

Frequency analysis ranges from 1 Hz to 20 kHz
Frequency accuracy is + 0.01 0/0 (Full scale)
Voltage ranges are + 1 mv – + 50 v.

Flow rate through the model turbine was measured by means of the bell mouth inlet from the plenum chamber. Construction of the bell mouth was based on BS1042 code and an inlet pipe was attached to it to calibrate it.

Flow rate was measured by making extensive velocity traverses in the inlet duct for various Reynold's numbers. The plane of measurement is shown in Figure 5. The velocity profiles were integrated graphically to obtain the flow rate. The expression for the same is $Q = 2\pi r dr Cz$. The calibration curve, flow rate vs. chamber pressure is shown in Figure 5. Total pressure is found by noting the value indicated by the central orifice of a three hole cylindrical probe. Before using the probe for measurements, it was calibrated. The difference in pressure between the central and one of the side orifices reads the dynamic pressure. The static pressure is found by wall static pressure tap and measured using the same. Comprehensive velocity traverses were taken at the exit of the turbine. The swirl angle θ is measured as a difference of the angle read by the protractor after balancing of the three hole probe and the reference angle. The reference angle is obtained during the calibration of the three hole probe. The two components of the velocity, the axial and the tangential velocity are evaluated as $C_z = C\cos\theta$, $C_\theta = C\sin\theta$, where C is the absolute velocity. The variation of C_z and C_θ is shown in Figure 6. The flow oscillations were measured using a hot wire probe at three locations in the draft tube, i.e. at A, B and C as shown in Figure 7. But for the present paper, the only important location of measurements is at station A. Hence, the results are discussed with reference to the same. The hot wire output signals were processed to give amplitude vs unit speed in Figure 8. The angular momentum parameter was evaluated using the expression $MD/\rho Q^2$, where M = rate of flow of angular momentum leaving the runner, D = diameter of runner = 0.15 m, Q = flow rate m^3/sec and ρ = density of air kg/m^3. M is computed from the traverse data.

$$M = \int_0^R 2\pi r dr C_z (rC_\theta),$$

$$M = \int_0^R 2\pi C_z C_\theta r^2 dr,$$

where r is the local radius, R is the radius of the duct, ρ is the density of fluid, and 0 represents the hub position.

The integration is carried out graphically by actually counting the squares under the curve to avoid computational error. $MD/\rho Q^2$ is a function of swirl, and swirl is a function of unit speed. Therefore, $MD/\rho Q^2$ is a function of unit speed. The variation of angular momentum parameter with unit speed is shown in Figure 9. The variation of velocity components C_z, C_θ is shown in Figure 6. C_z increases gradually towards the tip and then falls steadily. But for higher unit speeds of 125 rpm it

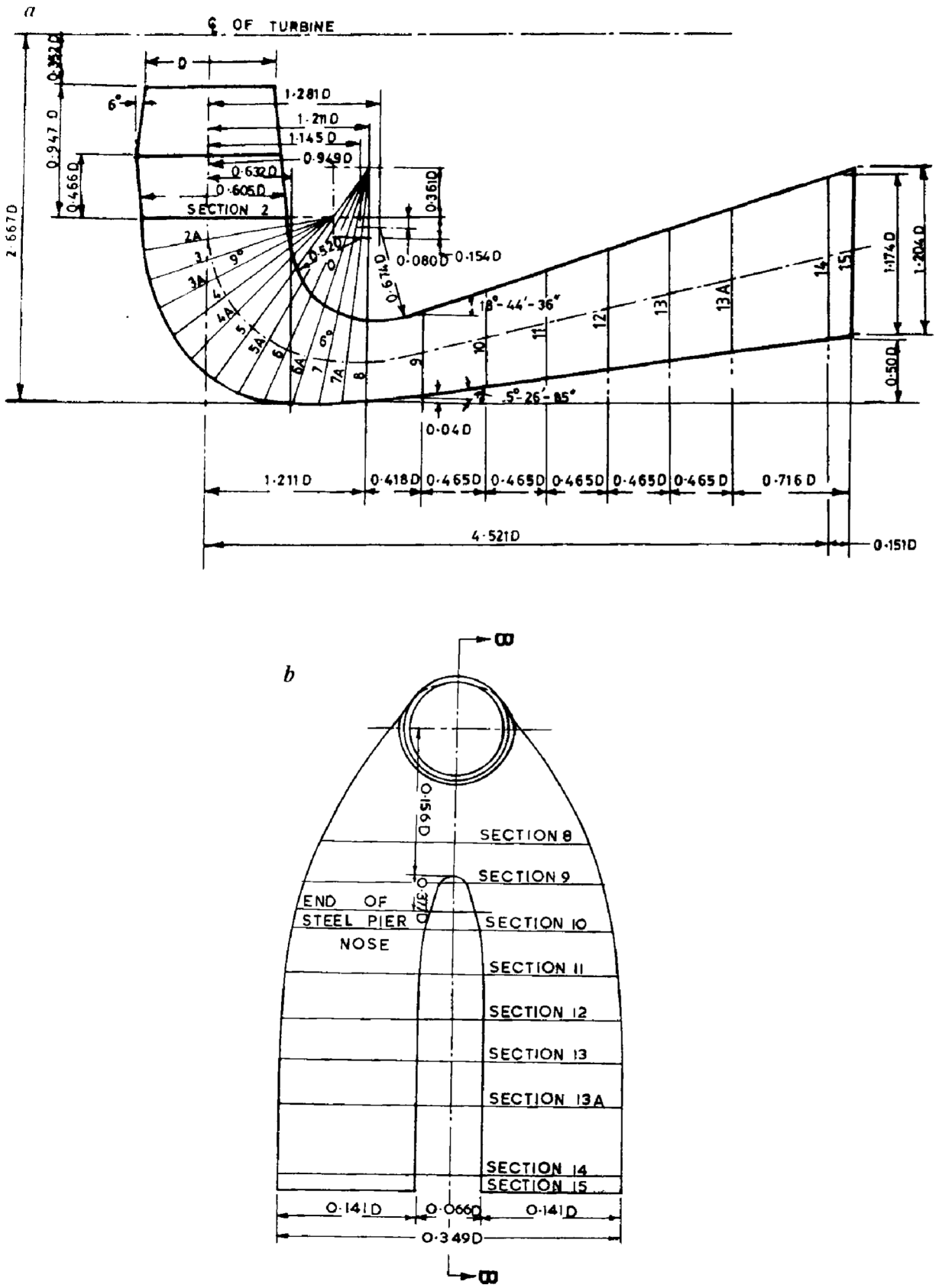

Figure 4. *a*, Elevation of draft tube; *b*. Plan of draft tube.

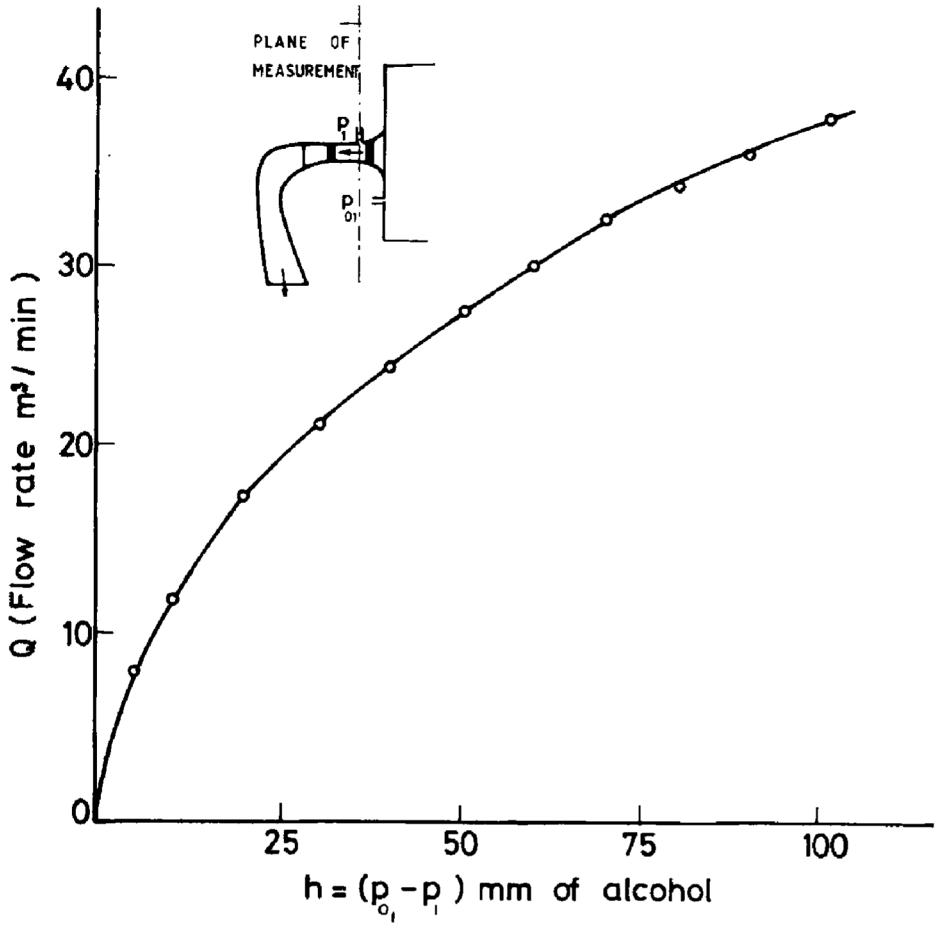

Figure 5. Calibration curve for inlet duct.

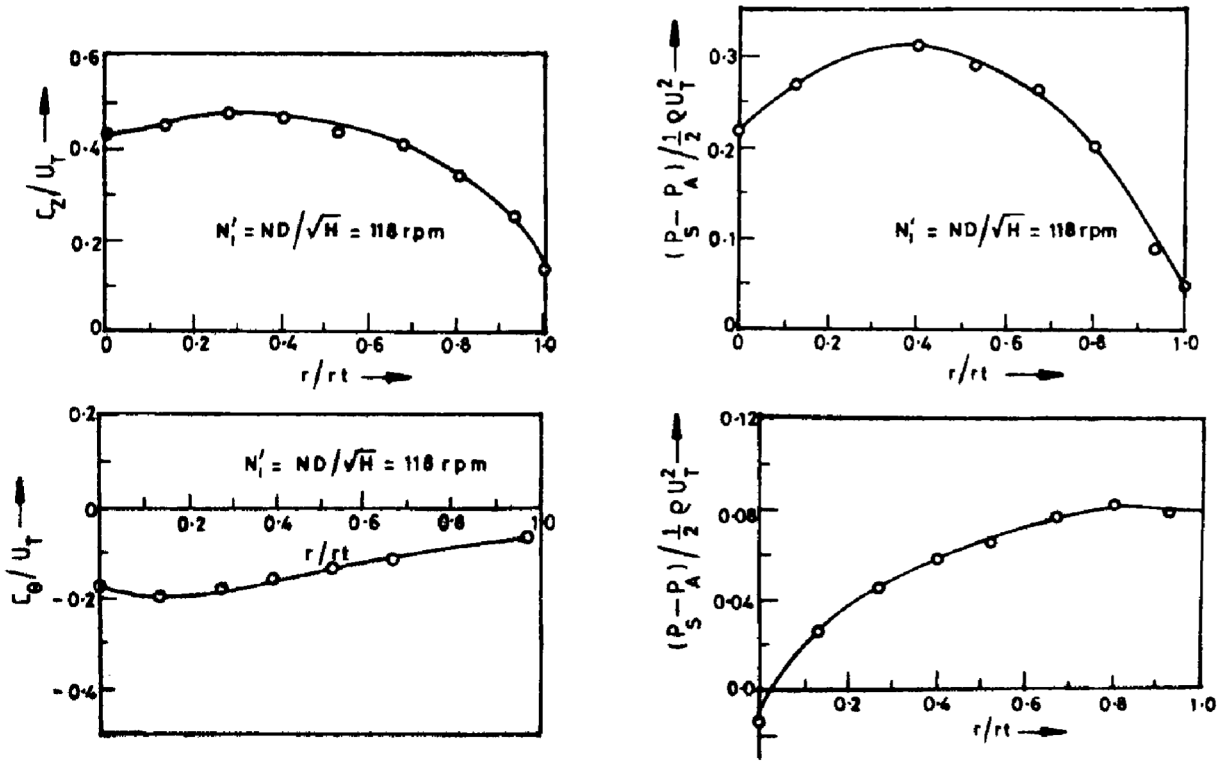

Figure 6 *a*. Variations of pressure and velocity downstream of impeller.

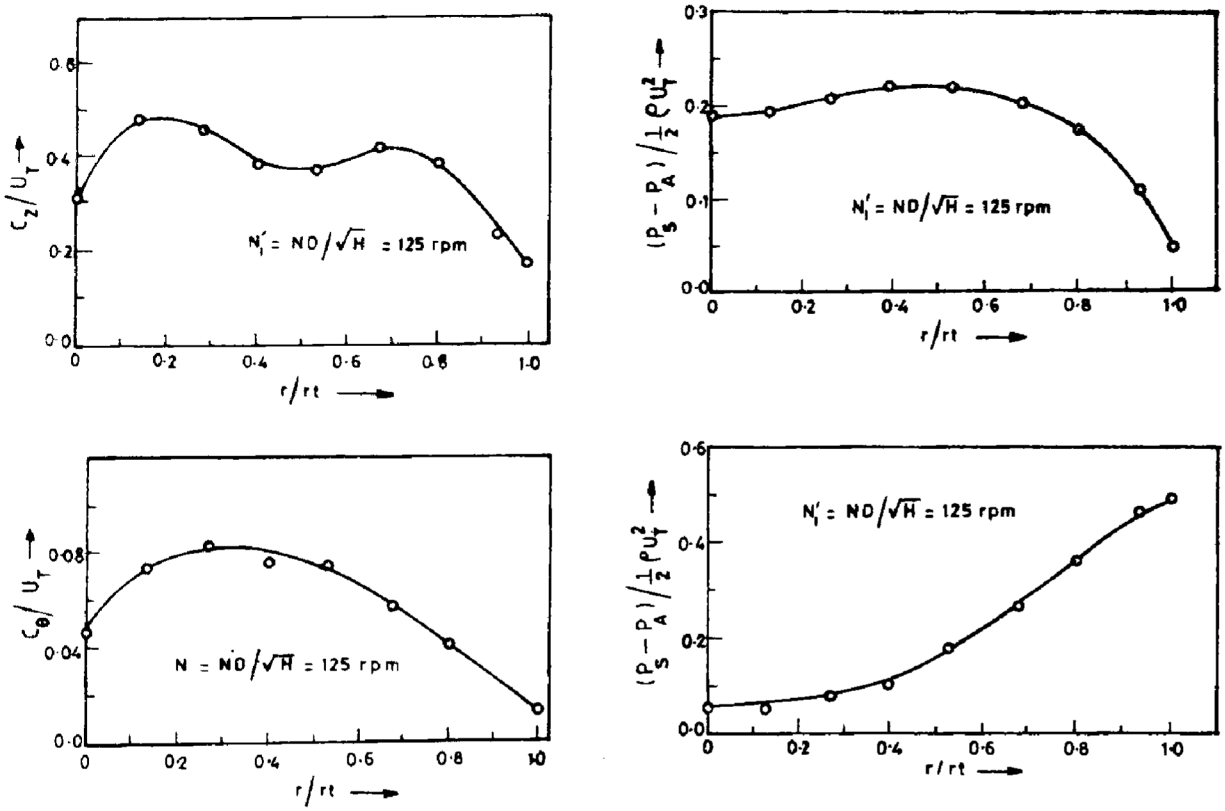

Figure 6 *b*. Variations of pressure and velocity downstream of impeller.

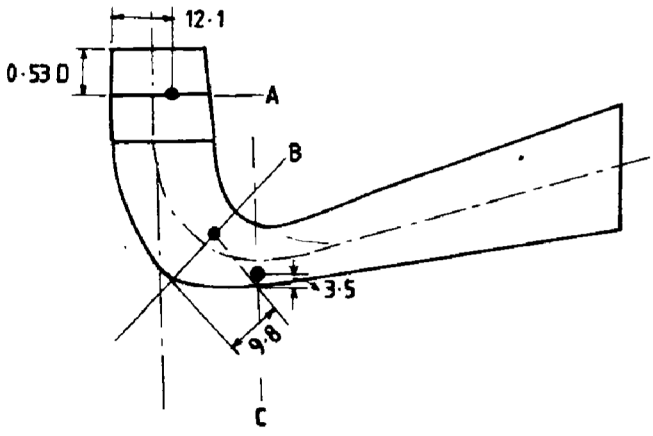

Figure 7. Position of measurements of oscillations.

slightly falls at mid span and then increases over an appreciable part of the blade and falls towards the tip. C_θ is wholly negative for the unit speed of 118 rpm. It increases for higher unit speed of 125 rpm. It is positive and increases up to $r/r_t = 0.3$ (r_t is the tip radius) and then falls steadily towards the tip. Total pressure increases up to $r/r_t = 0.4$, and then decreases while static pressure shows a steadily rising trend over the whole annulus as expected due to radial equilibrium equation $dp/dr = C_\theta/r$. It is seen that there is a very little distinction in the flow except at the clearly defined peak X, which refers to the runner rotational frequency (Figure 10 *a*). A decrease in the unit speed to 119 rpm shows the same spectrum as earlier with a rotational frequency X (Figure 10 *b*). When the unit speed is lowered further, the inlet angular momentum parameter is increased, and the presence of a disturbance Y at a frequency lower than the rotational frequency X is noticed (Figure 11 *a*). The frequency at Y is 0.49 times the rotational frequency, when the unit speed is lowered still further, to give a large inlet angular momentum parameter. There is a drastic increase in amplitude of the disturbance Y as seen in Figure 11 *b*. A further drop in the unit speed increases the disturbance Y which has an increased frequency of 0.639 times the rotational frequency (Figure 12 *a*). The same trend is seen when we increase the unit speed. So, at an increased unit speed of 220 rpm corresponding to disturbance frequency of 0.26 times the runner rotational frequency, again the disturbance is increased dramatically (Figure 12 *b*). This again shows the increased angular momentum parameter. It would be noticed that an increase in the disturbance amplitude has been accompanied by a drop in the amplitude of the signal at the rotational frequency. This is attributed to the fact that the vortex break down is of the spiral type. This is explained as follows. When there is no breakdown,

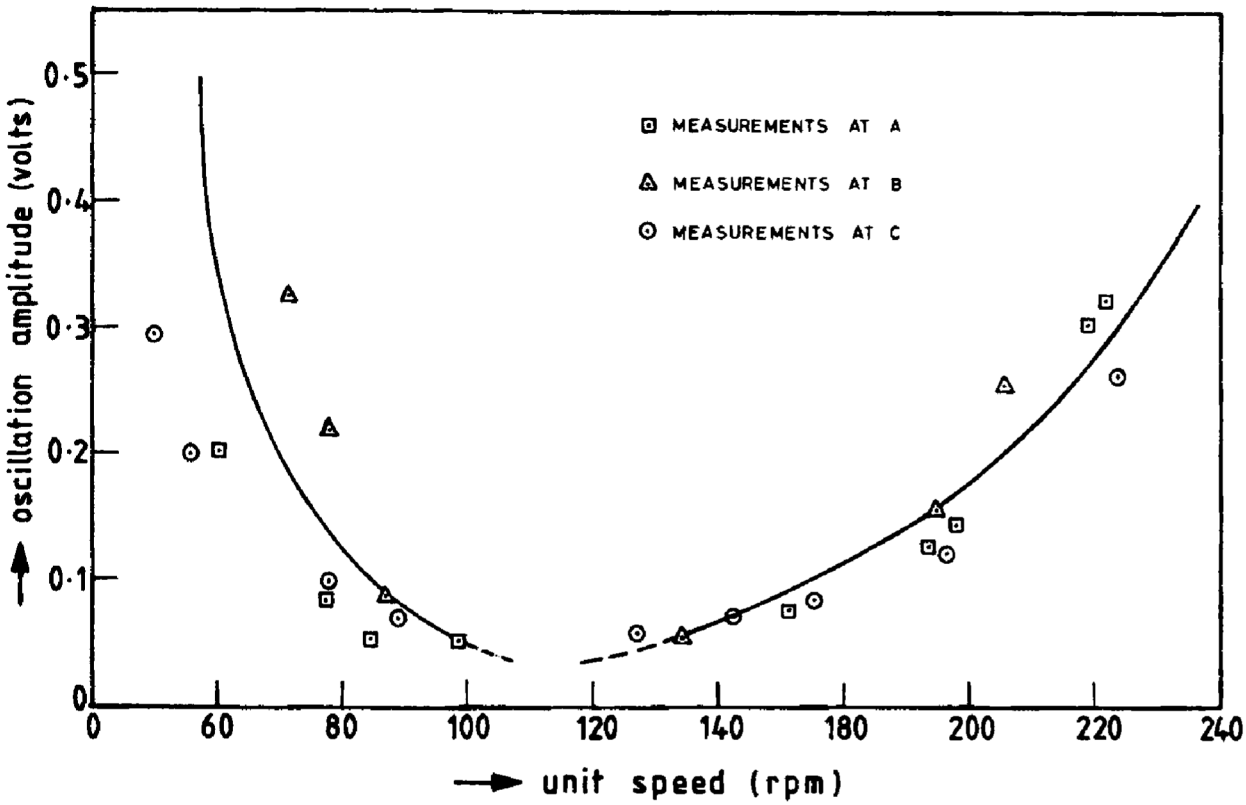

Figure 8. Variation of amplitude of flow oscillations with unit speed.

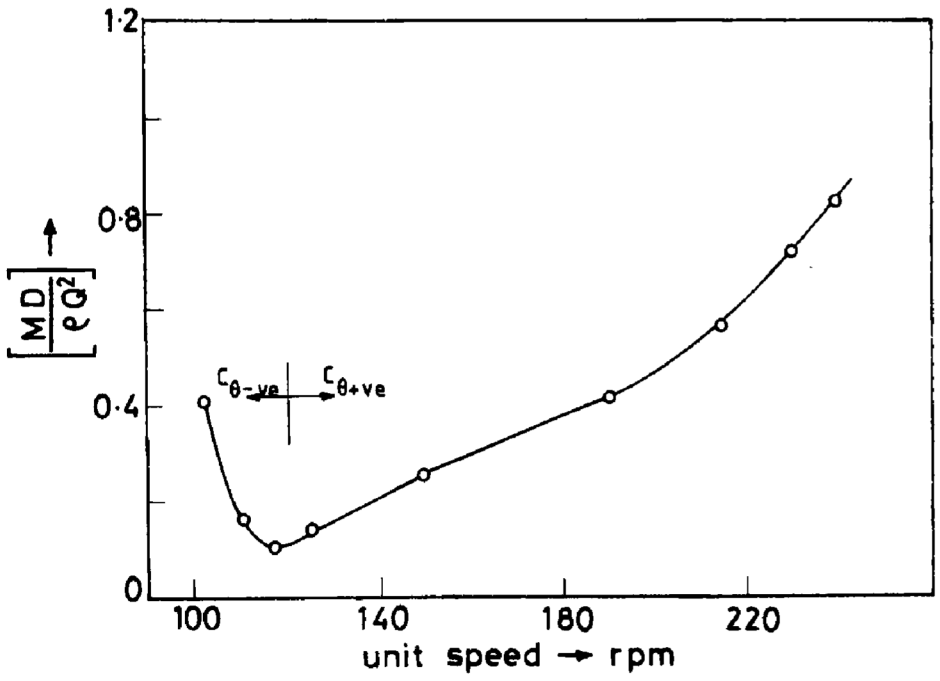

Figure 9. Variation of angular momentum parameter with unit speed.

the central vortex core is a straight rope composed of five individual strands of vortices emanating from each blade passage, possibly from the suction surface and hub corners. The rotation of this rope would give us a disturbance signal at the impeller frequency and a multiple of five times that value which would correspond to the blade passing frequency. Once the spiral breakdown occurs, the vortex would move off the centre line.

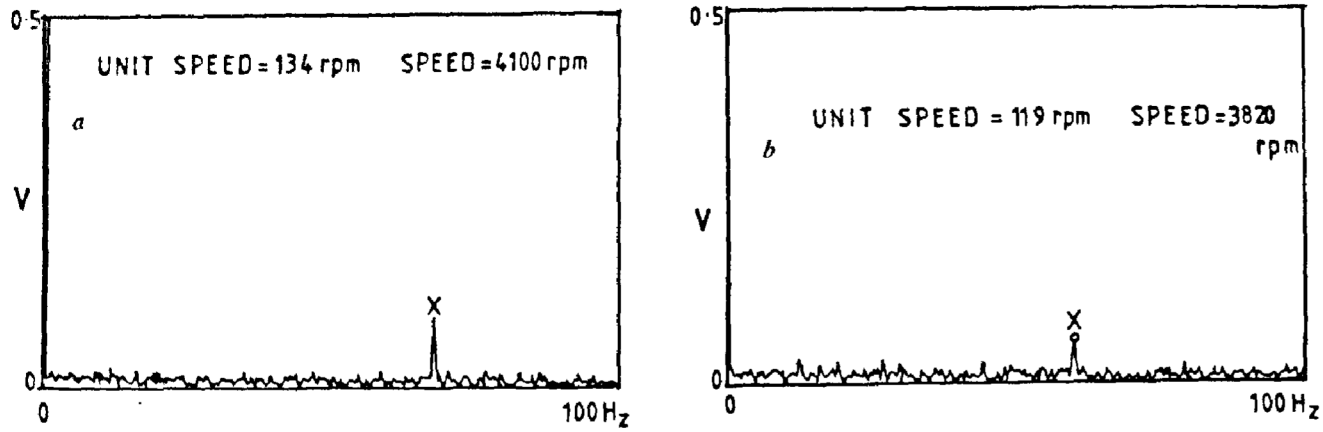

Figure 10.

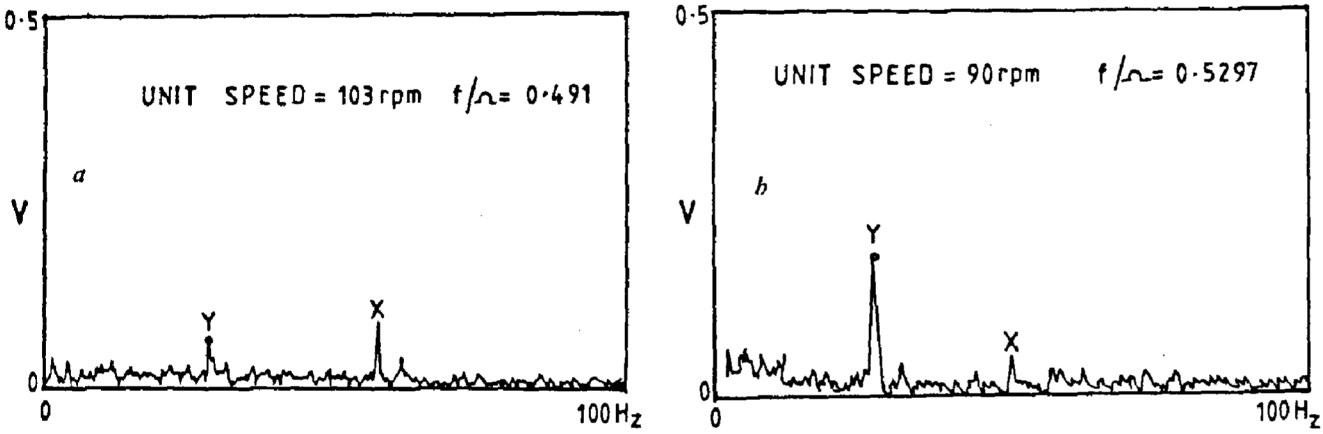

Figure 11.

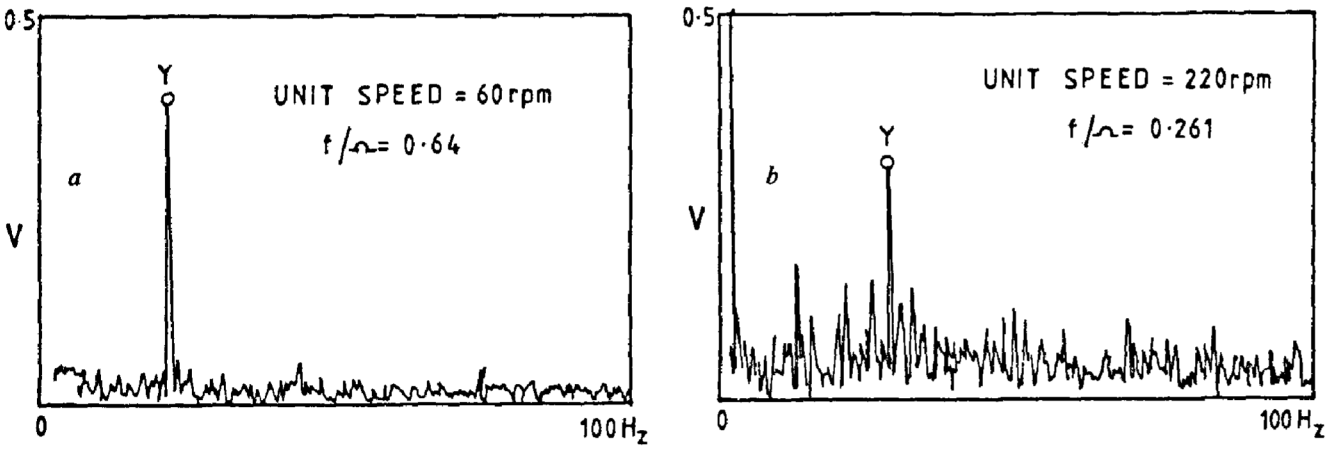

Figure 12.

Figures 10–12. Variation of disturbance frequency with unit speed.

Further, the regularity with which it had earlier got connected to the runner frequency and geometry would now be swamped by the displaced spiralling of the vortex following the breakdown. Figures 11 and 12 show the emergence of disturbing oscillations when the angular momentum parameter is above or below a narrow range. The range of the unit speed for which these disturbances are absent extend from 100 to 145 rpm. It will be seen that this corresponds to the lower portion of the momentum parameter curve around the turbine design point. Further, the variation of amplitude of oscillation versus the unit speed is shown in Figure 8. It is noted that the common feature of variation is an absence of a 'breakdown oscillation' in a narrow range of the unit

speed near the design point with a steady increase in oscillation outside the range accompanied by a large rise at the extreme ends. Another feature of variation is its close resemblance to the variation of angular momentum parameter with the unit speed. Oscillations seem to increase in steps of the angular momentum parameter.

However, in the design region the oscillations are absolute except downstream of the bend, where it seems to exist at very low level associated with possible spiralling of the core. Breakdown might have been rapid movement upstream of the spiralling core with a more or less rapid increase in its amplitude. Outside this range of the unit speed, i.e. at part and over load, flow oscillations occur at a well defined frequency. The magnitude of the oscillations increases as one moves away from the design point. The frequency of the oscillations is in the range 0.26–0.8 of the runner frequency. This coincides with the range of such oscillations noted in actual hydraulic turbines and is attributed to draft tube vortex breakdown, and it is also called draft tube surge. Undoubtedly, the observations in the present aerodynamic tests are carried by the same phenomenon. However, the pipe flow experiments have shown that the vortex breakdown is of an axi-symmetric type with stagnation bubble appearing on the centre line. One characteristic of axi-symmetric breakdown is the occurrence of two or more distinctive oscillation frequencies at the breakdown. The other type of breakdown is spiral type which is characterized by the presence of one dominating disturbance frequency (concluded from our observations, Figures 10–12). Hence, this leads us to postulate that the form of the breakdown in the present tests is the spiral type. This type of breakdown would be more or less forced by the presence of draft tube elbow and is identical to the spiralling rope pattern and is surely observed in the experiments on the cavitating runners at part and overload conditions. Cassidy[1] proposed that onset of the breakdown is defined by a critical angular momentum parameter given by $MD/\rho Q^2 = (1/95 \times L/D) + 0.295$. Taking the L/D ratio of our present draft tube as referring to the normalized length of the flow past we get $(MD/\rho Q^2)C = 0.388$. Judging from the appearance and the disappearance of the surge in the present tests it is possible to surmise that essentially surge-free operation occurs in a unit speed range of 105–150 rpm. From Figure 9 it will be seen that this corresponds to $(MD/\rho Q^2)C = 0.3$ above which draft tube oscillations are closely noticed. Obviously, the critical angular momentum parameter depends not only on the magnitude of $(MD/\rho Q^2)$ but also on the details of the way the swirl is distributed along the radius. It is worth mentioning that Cassidy's experiments were for nominally free vortex swirl variation at the entry, a situation that is rarely met within an actual turbine. Computational details of the flow are needed to further establish a close correlation between the angular momentum parameter and the initiation of vortex breakdown in draft tube flows.

1. Cassidy, J. J., Experimental study and analysis of draft tube surging, Report No. HYD-591, US Bureau of Reclamation, Colorodo, 1969.
2. Cassidy, J. J. and Falvey H. T., *J. Fluid Mech.*, 1970, **41**, 727.
3. Hall, H. G., *Annu. Rev. Fluid Mech.*, 1972, **4**, 195.
4. Harvey, J. K., *J. Fluid Mech.*, 1952, **14**, 585.
5. Sarpkaya, T., *J. Fluid Mech.*, 1971, **45**, 545.
6. Soundranayagam, S. and Mehata, R. C., Swirl at exit from water turbine runners and the effect on draft tube surge, 1979.
7. Squire, H. B., Imperial Coll. Sci. Technol., London, Report No. 102, 1960.
8. Palde, U. J., *IAHR Symposium*, Vienna, Paper 111/3, 1974.
9. Soundranayagam, S. and Sharma, C. L., International Conference on Fluid Machines, Paris, 1988.

Received 8 October 1997; revised accepted 21 October 1998